


Observation of New Ω_c^0 States Decaying to the $\Xi_c^+ K^-$ Final State

R. Aaij *et al.**
(LHCb Collaboration)

 (Received 10 February 2023; revised 26 April 2023; accepted 26 June 2023; published 26 September 2023)

Two new excited states, $\Omega_c(3185)^0$ and $\Omega_c(3327)^0$, are observed in the $\Xi_c^+ K^-$ invariant-mass spectrum using proton-proton collision data collected by the LHCb experiment, corresponding to an integrated luminosity of 9 fb^{-1} . Five previously observed excited Ω_c^0 states are confirmed, namely $\Omega_c(3000)^0$, $\Omega_c(3050)^0$, $\Omega_c(3065)^0$, $\Omega_c(3090)^0$, and $\Omega_c(3119)^0$. The masses and widths of these seven states are measured with the highest precision to date.

DOI: [10.1103/PhysRevLett.131.131902](https://doi.org/10.1103/PhysRevLett.131.131902)

Singly charmed baryons consist of one charm quark and two lighter quarks. Owing to the large mass difference between the charm quark and the lighter quarks, the singly charmed baryon mass spectrum can be described systematically in heavy quark effective theory (HQET) [1]. Many excited states are expected because of the complex interplay of the three-quark system, which makes them an ideal testing ground for theories of the strong force. Studies of charmed baryon spectroscopy have the potential to reveal important insights into the fundamental nature of hadronic matter.

In 2017, the LHCb collaboration reported the observation of five new narrow Ω_c^0 states decaying to the $\Xi_c^+ K^-$ final state [2]. Four of them have been confirmed in e^+e^- collisions by the Belle Collaboration [3] and in the $\Xi_c^+ K^-$ invariant-mass projection of $\Omega_b^- \rightarrow \Xi_c^+ K^- \pi^-$ decays by the LHCb Collaboration [4]. The inclusion of charge-conjugate processes is implied throughout this Letter, unless stated otherwise.

The Ω_c^0 states have been studied extensively from the theoretical side. Most theoretical studies interpret these states as excited bound states [5–21]; however, the different schemes for matching their masses and quantum numbers have resulted in conflicting interpretations among different studies. In some studies [22–24], the $\Omega_c(3050)^0$ and $\Omega_c(3090)^0$ states are interpreted as baryon-meson molecular (quasibound) states. Some theoretical studies [25,26] also suggest the presence of three pentaquark states ($sscq\bar{q}$) with masses very close to the $\Omega_c(3065)^0$, $\Omega_c(3090)^0$, and $\Omega_c(3119)^0$ states, which may indicate the presence of a considerable $sscq\bar{q}$ component in these three states.

In addition, another $sscq\bar{q}$ state is predicted with a mass of $\sim 2980 \text{ MeV}$ (natural units are used throughout this Letter). The branching fractions of excited Ω_c^0 baryons to final states such as $\Xi_c\pi$, $\Omega_c\eta$, etc., may depend on the internal molecular or pentaquark structure of these baryons, and thus provide a way to elucidate their inner structure. Furthermore, the search for new excited states is also an essential way to experimentally study the charmed baryon spectrum. A lattice QCD calculation [27] presents a rich invariant-mass spectrum; dozens of D - or F -wave excited states were identified, expanding our understanding of the charmed baryon spectrum. Studying the excited states of Ω_c^0 baryons provides a unique opportunity to explore the properties of these intriguing particles, and to examine and verify a variety of theoretical predictions, including phenomenological models, thereby deepening our understanding of fundamental strong interaction effects.

This Letter presents an updated analysis of the $\Xi_c^+ K^-$ invariant-mass spectrum, using proton-proton (pp) collision data collected by the LHCb experiment from 2011 to 2018 at center-of-mass energies of 7, 8, and 13 TeV, corresponding to integrated luminosities of 1, 2, and 6 fb^{-1} , respectively. Grouped by trigger strategy, data recorded in 2011–2015 is referred to as dataset 1, and data collected in 2016–2018 is referred to as dataset 2. The increased charm production cross section at higher center-of-mass energy, the higher integrated luminosity, and the improvement in the trigger system [28,29] result in a 5 times larger sample size compared with the previous analysis [2]. The results presented in this Letter supersede the previous mass and width determinations [2].

The LHCb detector [30,31] is a single-arm forward spectrometer covering the pseudorapidity range $2 < \eta < 5$, designed for the study of particles containing b or c quarks. Simulated data samples are produced with the software packages described in Refs. [32–36] and are used to develop the event selection, estimate the invariant-mass resolution, and model physics processes that may constitute peaking backgrounds in the analysis.

*Full author list given at the end of the Letter.

Published by the American Physical Society under the terms of the [Creative Commons Attribution 4.0 International license](https://creativecommons.org/licenses/by/4.0/). Further distribution of this work must maintain attribution to the author(s) and the published article's title, journal citation, and DOI. Funded by SCOAP³.

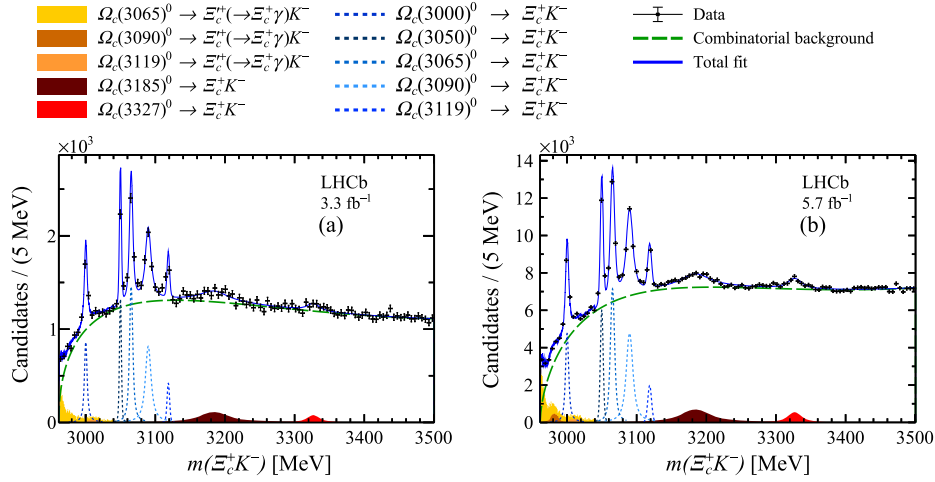


FIG. 1. Invariant-mass distribution of the $\Omega_c(X)^0$ candidates in (a) dataset 1 and (b) dataset 2, with the fit results overlaid. A bin width of 5 MeV is used for plotting. The previously observed excited Ω_c^0 states are shown in blue dashed lines. The $\Omega_c(3185)^0$ state is shown in the brown area, and the $\Omega_c(3327)^0$ state is shown in the red area. Three feed-down components are shown as the yellow areas, while the green long-dashed line corresponds to the combinatorial background.

The $\Xi_c^+(\rightarrow pK^-\pi^+)$ candidates are formed with three tracks that do not originate from any primary pp interaction vertex (PV) and have significant transverse momentum (p_T). Particle identification (PID) requirements are applied to all the final-state tracks in order to suppress combinatorial background. Additionally, PID vetoes are applied to suppress background from misidentified charm meson decays. These vetoes are formed by placing requirements on the invariant mass of the candidates recomputed with the relevant change in the particle mass hypothesis. The Ξ_c^+ candidates are required to have a large flight-distance significance from any PV and a small value of χ_{IP}^2 , defined as the difference between the vertex fit χ^2 of the PV reconstructed with and without the particle in question. The reconstructed Ξ_c^+ candidates must have an invariant mass in the range of [2450, 2485] MeV, corresponding to about 3 times the invariant-mass resolution around the known Ξ_c^+ mass [37]. Each Ξ_c^+ candidate is combined with a K^- candidate that originates from the same PV and has p_T greater than 0.4 GeV. The $\Xi_c^+ K^-$ combinations with good vertex quality and p_T greater than 4.5 GeV are retained as $\Omega_c(X)^0$ candidates, where X is the mass of the excited state.

A multivariate classifier based on a boosted decision tree (BDT) algorithm [38] and implemented in the TMVA [39] toolkit is used to further improve the signal purity. The variables used to train the BDT classifier are the χ^2 value of the Ξ_c^+ decay-vertex fit; the Ξ_c^+ flight distance; the angle between the Ξ_c^+ momentum vector and the line that connects the Ξ_c^+ decay vertex with its PV; the χ_{IP}^2 and p_T of Ξ_c^+ and $\Omega_c(X)^0$ candidates; and the χ_{IP}^2 , p_T and particle-identification variables of all final state particles. Owing to the difference in trigger strategies, different BDT classifiers are used for datasets 1 and 2. The BDT classifier is trained with simulated signal decays generated with the

2012 (2016) configuration for dataset 1 (dataset 2), and background candidates taken from the Ξ_c^+ invariant-mass sideband region, defined as [2400, 2440] MeV and [2500, 2540] MeV. The working points are chosen such that the BDT classifier efficiency on the signal is 75%; no fine-tuned optimization is performed to avoid favoring any particular excited state.

To improve the mass resolution, the variable $m(\Xi_c^+ K^-)$ is defined as the difference between the invariant mass of the $\Omega_c(X)^0$ and Ξ_c^+ candidates, to which the known Ξ_c^+ mass [37] is added. The $\Xi_c^+ K^-$ invariant-mass distribution is shown in Fig. 1, where seven peaking structures are seen. Five of them have been observed in the previous analysis [2], while the $\Omega_c(3185)^0$ and $\Omega_c(3327)^0$ states are observed for the first time. There are no similar structures in the wrong-sign sample ($\Xi_c^+ K^+$) or in the spectrum of Ξ_c^+ sideband candidates combined with a kaon.

To determine the masses and widths of these $\Omega_c(X)^0$ states, an extended maximum likelihood fit with bin widths of 1 MeV is performed to the $\Xi_c^+ K^-$ invariant-mass distributions, simultaneously to datasets 1 and 2. The $\Omega_c(X)^0$ contributions are described by S -wave relativistic Breit–Wigner functions convolved with a Gaussian resolution function whose width is determined from simulated signal samples. The combinatorial background is parametrized by an empirical function,

$$B(\Delta m) = (\Delta m)^a \times \exp(b_1 \Delta m + b_2 \Delta m^2), \quad (1)$$

where Δm is the difference between the invariant mass of the $\Xi_c^+ K^-$ candidate and the $\Xi_c^+ K^-$ mass threshold, and a , b_1 , and b_2 are free parameters. In addition, three feed-down components from partially reconstructed decays of the $\Omega_c(3065)^0$, $\Omega_c(3090)^0$, and $\Omega_c(3119)^0$ resonances are

TABLE I. Fit results of the mass, width, and yield for each state, and for each data set. Uncertainties are statistical only.

Resonance	m (MeV)	Γ (MeV)	Yield (dataset 1)	Yield (dataset 2)
$\Omega_c(3000)^0$	3000.44 ± 0.07	3.83 ± 0.23	1225 ± 83	7533 ± 263
$\Omega_c(3050)^0$	3050.18 ± 0.04	0.67 ± 0.17	1139 ± 65	7379 ± 215
$\Omega_c(3065)^0$	3065.63 ± 0.06	3.79 ± 0.20	2180 ± 99	13046 ± 316
$\Omega_c(3090)^0$	3090.16 ± 0.11	8.48 ± 0.44	2234 ± 136	14434 ± 486
$\Omega_c(3119)^0$	3118.98 ± 0.12	0.60 ± 0.63	470 ± 66	3279 ± 234
$\Omega_c(3185)^0$	3185.1 ± 1.7	50 ± 7	1642 ± 367	10278 ± 1565
$\Omega_c(3327)^0$	3327.1 ± 1.2	20 ± 5	489 ± 173	3649 ± 723

included. These contributions are from $\Omega_c(X)^0 \rightarrow \Xi_c^+(\rightarrow \Xi_c^+\gamma)K^-$ decays, where the photon is not reconstructed. Their shapes are determined from simulated samples and are fixed, while their yields are free to vary in the fit.

The fit results are shown in Fig. 1 and summarized in Table I. In addition to the five narrow states at lower invariant mass that were previously observed, two new states with masses of about 3185 MeV and 3327 MeV, denoted $\Omega_c(3185)^0$ and $\Omega_c(3327)^0$ are observed with high significance.

The enhancement around the $\Xi_c^+K^-$ mass threshold is described by the partially reconstructed decays of $\Omega_c(X)^0 \rightarrow \Xi_c^+(\rightarrow \Xi_c^+\gamma)K^-$, as was done in the previous analysis [2]. In the exclusive analysis using the $\Omega_b^- \rightarrow \Omega_c(X)^0(\rightarrow \Xi_c^+K^-)\pi^-$ decay [4], these feed-down components are excluded by requiring an appropriate signal mass window of the Ω_b^- baryon, while the threshold enhancement is still present. This enhancement was modeled as an S -wave Breit-Wigner distribution, but the available data in Ref. [4] are not sufficient to declare an observation. To check if this resonance structure is present in this analysis, the enhancement is fitted using two alternative models: a Breit-Wigner component with and without the feed down coming from the $\Omega_c(3065)^0$ contribution. The yield of the $\Omega_c(3065)^0$ feed down is constrained to be 10% of the $\Omega_c(3065)^0$ signal yield for the former. This constraint is equivalent to fixing the ratio $\mathcal{B}[\Omega_c(3065)^0 \rightarrow \Xi_c^+K^-] \times \mathcal{B}(\Xi_c^+ \rightarrow \Xi_c^+\gamma) / \mathcal{B}[\Omega_c(3065)^0 \rightarrow \Xi_c^+K^-]$ to 0.1, which is chosen due to the small phase space of the $\Omega_c(3065)^0 \rightarrow \Xi_c^+K^-$ decay. The yields of the other feed-down contributions are free to float. Unfortunately, the shape of the $\Omega_c(3065)^0$ feed down and the additional Breit-Wigner structure are too similar to be separated in this analysis. The relative contributions from these two components cannot be determined from data, and hence this is accounted for as a systematic uncertainty. The existence of another hidden state cannot be excluded.

The mass difference between the $\Omega_c(3185)^0$ and $\Omega_c(3327)^0$ baryons is approximately the mass of the pion. It is possible that partially reconstructed candidates from the $\Omega_c(3327)^0$ decay fall into the $\Omega_c(3185)^0$ region,

such as $\Omega_c(3327)^0 \rightarrow \Xi_c(2645)^+(\rightarrow \Xi_c^+\pi^0)K^-$ and $\Omega_c(3327)^0 \rightarrow \Xi_c^+(\rightarrow \Xi_c^+\gamma)K^-$ decays with the π^0 or γ not reconstructed. The $m(\Xi_c^+K^-)$ line shapes of such contributions are obtained using the fast simulation toolkit RapidSim [40]. The feed-down contributions have been studied under different spin structure hypotheses, and differences from phase-space simulation were found to be negligible. The fit favors the presence of the $\Omega_c(3327)^0$ feed down with the π^0 missing. The $\Omega_c(3327)^0$ feed down strongly affects the measured mass and width of the $\Omega_c(3185)^0$ baryon, and is assigned as a systematic uncertainty. None of the models for the $\Omega_c(3185)^0$ region can be ruled out. In addition, the effects of the three-body decay $\Omega_c(3327)^0 \rightarrow \Xi_c^+K^-\pi^0$ are checked with a uniform phase-space model, and found to be insignificant on any of the states when assuming the ratio $\mathcal{B}[\Omega_c(3327)^0 \rightarrow \Xi_c^+K^-\pi^0] / \mathcal{B}[\Omega_c(3327)^0 \rightarrow \Xi_c^+K^-]$ to be unity.

The effects of the $\Xi_c(3055)^0 \rightarrow \Xi_c^+(\rightarrow \Xi_c^+\gamma)\pi^-$, $\Xi_c(3055)^0 \rightarrow \Xi_c(2645)^+(\rightarrow \Xi_c^+\pi^0)\pi^-$, and $\Xi_c(2923/2939/2965)^0 \rightarrow \Xi_c^+\pi^-$ decays, for which the pion is misidentified as a kaon and the π^0/γ from the $\Xi_c(2645)^+/\Xi_c^+$ decays is missing, are studied and found to be negligible. The contribution from $\Omega_c(3327)^0 \rightarrow \Xi_c^+K^{*-}$ is kinematically suppressed.

Several checks are performed to confirm the existence of the observed states and the stability of the fitted parameters. Each dataset is divided into subsamples according to data-taking conditions, charge combination ($\Xi_c^+K^-$ or $\Xi_c^-K^+$), or different intervals of $p_T(K^-)$ and $p_T(\Xi_c^+)$. In all tests, the results are consistent with the default fit. A two-peak structure also describes the data well in the mass region around 3185 MeV; hence, the presence of two states in this region cannot be excluded. The bias from the fit model itself is estimated using pseudoexperiments. For each parameter, the mean differences between the fitted values and the input ones are included as systematic uncertainties.

The uncertainty related to the signal model is estimated by fitting the data with variations in the spin hypotheses and the Blatt-Weisskopf factor [41]. The systematic uncertainty from the combinatorial background model is estimated by using a fourth-order Chebyshev polynomial as an

TABLE II. Systematic uncertainties on the measured masses and natural widths.

Source (MeV, MeV)	$\Omega_c(3000)^0$ [m, Γ]	$\Omega_c(3050)^0$ [m, Γ]	$\Omega_c(3065)^0$ [m, Γ]	$\Omega_c(3090)^0$ [m, Γ]	$\Omega_c(3119)^0$ [m, Γ]	$\Omega_c(3185)^0$ [m, Γ]	$\Omega_c(3327)^0$ [m, Γ]
Threshold structure	[+0.01, +1.23] [-0.07, -0.19]	[+0.00, +0.00] [-0.01, -0.17]	[+0.01, +0.00] [-0.00, -0.11]	[+0.01, +0.12] [-0.00, -0.20]	[+0.06, +0.00] [-0.00, -0.16]	[+0.32, +8.05] [-0.57, -0.83]	[+0.01, +1.71] [-0.15, -0.04]
Feed down from $\Omega_c^0(3327)$	[+0.04, +0.04] [-0.00, -0.00]	[+0.00, +0.00] [-0.00, -0.01]	[+0.01, +0.03] [-0.00, -0.00]	[+0.01, +0.22] [-0.00, -0.00]	[+0.01, +0.07] [-0.00, -0.00]	[+4.28, +0.00] [-0.00, -10.81]	[+0.00, +0.98] [-0.20, -0.00]
Fit bias	[+0.02, +0.01] [-0.00, -0.00]	[+0.02, +0.12] [-0.00, -0.00]	[+0.00, +0.08] [-0.00, -0.00]	[+0.01, +0.20] [-0.00, -0.00]	[+0.00, +0.40] [-0.02, -0.00]	[+0.00, +4.84] [-0.37, -0.00]	[+0.00, +0.00] [-0.18, -0.70]
Spin and radius	[+0.01, +0.01] [-0.01, -0.01]	[+0.01, +0.01] [-0.01, -0.01]	[+0.01, +0.02] [-0.01, -0.01]	[+0.01, +0.05] [-0.01, -0.01]	[+0.01, +0.06] [-0.01, -0.01]	[+0.01, +0.56] [-0.18, -0.01]	[+0.01, +0.01] [-0.02, -0.60]
Background	[+0.04, +0.98] [-0.00, -0.00]	[+0.00, +0.00] [-0.01, -0.18]	[+0.00, +0.00] [-0.00, -0.29]	[+0.00, +0.00] [-0.06, -1.58]	[+0.00, +0.00] [-0.21, -0.60]	[+5.98, +0.00] [-0.00, -16.2]	[+0.00, +12.9] [-1.24, -0.00]
Bin size	[+0.00, +0.06] [-0.10, -0.04]	[+0.00, +0.40] [-0.01, -0.03]	[+0.02, +0.08] [-0.03, -0.07]	[+0.01, +0.37] [-0.05, -0.09]	[+0.00, +0.00] [-0.06, -0.60]	[+0.14, +2.75] [-0.48, -0.50]	[+0.07, +1.16] [-0.00, -0.00]
Momentum calibration	[$\pm 0.01, \dots$]	[$\pm 0.03, \dots$]	[$\pm 0.03, \dots$]	[$\pm 0.04, \dots$]	[$\pm 0.05, \dots$]	[$\pm 0.07, \dots$]	[$\pm 0.11, \dots$]
Energy loss	[$\pm 0.04, \dots$]	[$\pm 0.04, \dots$]	[$\pm 0.04, \dots$]	[$\pm 0.04, \dots$]	[$\pm 0.04, \dots$]	[$\pm 0.04, \dots$]	[$\pm 0.04, \dots$]
Simulation/Data difference	[+0.00, +0.20] [-0.01, -0.22]	[+0.01, +0.48] [-0.04, -0.67]	[+0.01, +0.36] [-0.00, -0.35]	[+0.00, +0.36] [-0.02, -0.29]	[+0.03, +0.80] [-0.00, -0.59]	[+0.08, +2.58] [-0.34, -0.67]	[+0.02, +0.27] [-0.05, -0.28]
Total	[+0.07, +1.59] [-0.13, -0.29]	[+0.06, +0.64] [-0.07, -0.72]	[+0.06, +0.38] [-0.06, -0.47]	[+0.06, +0.61] [-0.10, -1.62]	[+0.09, +0.90] [-0.23, -1.05]	[+7.36, +10.1] [-0.92, -19.5]	[+0.14, +13.1] [-1.28, -0.96]

alternative function. In addition, a systematic uncertainty is assigned based on the spread of results obtained by performing the fit with different bin widths.

Some sources of systematic uncertainty only contribute to the mass measurement, including the momentum calibration for charged particles, which has a relative accuracy of 0.03% [42,43], and the energy loss due to the imperfect modeling of the detector material, which results in a 0.04 MeV uncertainty. The differences between simulation and data mainly affect the measurement of the natural width of each state. It is calculated by varying the width of the resolution function by 10% [44]. Other assumptions for the $\Omega_c(3185)^0$ structure, such as the two-peak structure, additional feed-down components, or a combination of the two-peak structure and one more feed-down assumption cannot be excluded, and are included in the systematic uncertainties.

The systematic uncertainties are summarized in Table II. After considering the systematic uncertainty, the

 TABLE III. Measured mass and natural width for each of the seven $\Omega_c(X)^0$ states. The first uncertainty is statistical, and the second is systematic; the third (mass only) arises from the uncertainty of the known Ξ_c^+ mass.

Resonance	m (MeV)	Γ (MeV)
$\Omega_c(3000)^0$	$3000.44 \pm 0.07^{+0.07}_{-0.13} \pm 0.23$	$3.83 \pm 0.23^{+1.59}_{-0.29}$
$\Omega_c(3050)^0$	$3050.18 \pm 0.04^{+0.06}_{-0.07} \pm 0.23$	$0.67 \pm 0.17^{+0.64}_{-0.72}$ < 1.8 MeV, 95% CL
$\Omega_c(3065)^0$	$3065.63 \pm 0.06^{+0.06}_{-0.06} \pm 0.23$	$3.79 \pm 0.20^{+0.38}_{-0.47}$
$\Omega_c(3090)^0$	$3090.16 \pm 0.11^{+0.06}_{-0.10} \pm 0.23$	$8.48 \pm 0.44^{+0.61}_{-1.62}$
$\Omega_c(3119)^0$	$3118.98 \pm 0.12^{+0.09}_{-0.23} \pm 0.23$	$0.60 \pm 0.63^{+0.90}_{-1.05}$ < 2.5 MeV, 95% CL
$\Omega_c(3185)^0$	$3185.1 \pm 1.7^{+7.4}_{-0.9} \pm 0.2$	$50 \pm 7^{+10}_{-20}$
$\Omega_c(3327)^0$	$3327.1 \pm 1.2^{+0.1}_{-1.3} \pm 0.2$	$20 \pm 5^{+13}_{-1}$

significance of the $\Omega_c(3185)^0$ and $\Omega_c(3327)^0$ states is larger than 12σ and 10σ , respectively. The significance for each state is determined from Wilk's theorem using the difference in log-likelihood with and without that signal component. The results of the measured mass and natural width of all seven states, shown in Table III, are the most precise to date, and supersede those in Ref. [2]. The correlations between these results and those in Ref. [4] are negligible, except for the systematic uncertainty due to the momentum calibration and energy loss, which are fully correlated. The natural widths of the $\Omega_c(3050)^0$ and $\Omega_c(3119)^0$ baryons are very close to zero; therefore upper limits on them are set at Bayesian 95% confidence level (CL), assuming Gaussian behavior for both statistical and systematic uncertainties.

In conclusion, the $\Xi_c^+ K^-$ invariant-mass spectrum is investigated using pp collision data collected by the LHCb experiment. With a total integrated luminosity of 9 fb^{-1} , we were able to select a high-purity sample of Ξ_c^+ candidates and observe seven excited states, including two that had never been seen before: the $\Omega_c(3185)^0$ and $\Omega_c(3327)^0$ states, and also the $\Omega_c(3119)^0$ state that is not seen in the exclusive analysis using the $\Omega_b^- \rightarrow \Omega_c(X)^0 (\rightarrow \Xi_c^+ K^-) \pi^-$ decay [4]. The $\Omega_c(3185)^0$ and $\Omega_c(3327)^0$ states have masses close to the threshold of the ΞD and ΞD^* final states. Referring to the lattice QCD result of Ref. [27], the $\Omega_c(3185)^0$ mass is in the predicted range for P -wave states, and the $\Omega_c(3327)^0$ mass is in the range for many possible states. While the quantum numbers of these states remain to be determined, their observations provide new information on the complex hadron spectroscopy in order to develop a deeper understanding of the strong interaction and its underlying principles.

We express our gratitude to our colleagues in the CERN accelerator departments for the excellent performance of the

LHC. We thank the technical and administrative staff at the LHCb institutes. We acknowledge support from CERN and from the national agencies: CAPES, CNPq, FAPERJ and FINEP (Brazil); MOST and NSFC (China); CNRS/IN2P3 (France); BMBF, DFG, and MPG (Germany); INFN (Italy); NWO (Netherlands); MNiSW and NCN (Poland); MEN/IFA (Romania); MICINN (Spain); SNSF and SER (Switzerland); NASU (Ukraine); STFC (United Kingdom); DOE NP and NSF (USA). We acknowledge the computing resources that are provided by CERN, IN2P3 (France), KIT and DESY (Germany), INFN (Italy), SURF (Netherlands), PIC (Spain), GridPP (United Kingdom), CSCS (Switzerland), IFIN-HH (Romania), CBPF (Brazil), Polish WLCG (Poland), and NERSC (USA). We are indebted to the communities behind the multiple open-source software packages on which we depend. Individual groups or members have received support from ARC and ARDC (Australia); Minciencias (Colombia); AvH Foundation (Germany); EPLANET, Marie Skłodowska-Curie Actions and ERC (European Union); A*MIDEX, ANR, IPhU and Labex P2IO, and Région Auvergne-Rhône-Alpes (France); Key Research Program of Frontier Sciences of CAS, CAS PIFI, CAS CCEPP, Fundamental Research Funds for the Central Universities, and Sci. & Tech. Program of Guangzhou (China); GVA, XuntaGal, GENCAT and Prog. Atracción Talento, CM (Spain); SRC (Sweden); and the Leverhulme Trust, the Royal Society and UKRI (United Kingdom).

-
- [1] A. G. Grozin, Introduction to the heavy quark effective theory. part 1, [arXiv:hep-ph/9908366](https://arxiv.org/abs/hep-ph/9908366).
- [2] R. Aaij *et al.* (LHCb Collaboration), Observation of Five New Narrow Ω_c^0 States Decaying to $\Xi_c^+ K^-$, *Phys. Rev. Lett.* **118**, 182001 (2017).
- [3] J. Yelton *et al.* (Belle Collaboration), Observation of excited Ω_c charmed baryons in e^+e^- collisions, *Phys. Rev. D* **97**, 051102 (2018).
- [4] R. Aaij *et al.* (LHCb Collaboration), Observation of excited Ω_c^0 baryons in $\Omega_b^- \rightarrow \Xi_c^+ K^- \pi^+$ decays, *Phys. Rev. D* **104**, L091102 (2021).
- [5] M. Karliner and J. L. Rosner, Very narrow excited Ω_c baryons, *Phys. Rev. D* **95**, 114012 (2017).
- [6] H.-X. Chen, Q. Mao, W. Chen, A. Hosaka, X. Liu, and Shi-Lin Zhu, Decay properties of P -wave charmed baryons from light-cone QCD sum rules, *Phys. Rev. D* **95**, 094008 (2017).
- [7] K.-L. Wang, L.-Y. Xiao, X.-H. Zhong, and Q. Zhao, Understanding the newly observed Ω_c states through their decays, *Phys. Rev. D* **95**, 116010 (2017).
- [8] W. Wang and R.-L. Zhu, Interpretation of the newly observed Ω_c^0 resonances, *Phys. Rev. D* **96**, 014024 (2017).
- [9] H.-Y. Cheng and C.-W. Chiang, Quantum numbers of Ω_c states and other charmed baryons, *Phys. Rev. D* **95**, 094018 (2017).
- [10] Z. Zhao, D.-D. Ye, and A. Zhang, Hadronic decay properties of newly observed Ω_c baryons, *Phys. Rev. D* **95**, 114024 (2017).
- [11] S. S. Agaev, K. Azizi, and H. Sundu, Interpretation of the new Ω_c^0 states via their mass and width, *Eur. Phys. J. C* **77**, 395 (2017).
- [12] B. Chen and X. Liu, New Ω_c^0 baryons discovered by LHCb as the members of $1P$ and $2S$ states, *Phys. Rev. D* **96**, 094015 (2017).
- [13] Z.-G. Wang, Analysis of $\Omega_c(3000)$, $\Omega_c(3050)$, $\Omega_c(3066)$, $\Omega_c(3090)$ and $\Omega_c(3119)$ with QCD sum rules, *Eur. Phys. J. C* **77**, 325 (2017).
- [14] K.-L. Wang, Y.-X. Yao, X.-H. Zhong, and Q. Zhao, Strong and radiative decays of the low-lying S - and P -wave singly heavy baryons, *Phys. Rev. D* **96**, 116016 (2017).
- [15] Y.-X. Yao, K.-L. Wang, and X.-H. Zhong, Strong and radiative decays of the low-lying D -wave singly heavy baryons, *Phys. Rev. D* **98**, 076015 (2018).
- [16] Q. Mao, H. X. Chen, A. Hosaka, X. Liu, and S. L. Zhu, D -wave heavy baryons of the $SU(3)$ flavor 6_F , *Phys. Rev. D* **96**, 074021 (2017).
- [17] E. Santopinto, A. Giachino, J. Ferretti, H. García-Tecocoatzí, M. A. Bedolla, R. Bijker, and E. Ortiz-Pacheco, The Ω_c -puzzle solved by means of quark model predictions, *Eur. Phys. J. C* **79**, 1012 (2019).
- [18] H.-g. Xu, G. Chen, Y. L. Yan, D. M. Zhou, L. Zheng, Y. L. Xie, Z. L. She, and B. H. Sa, Study on the Ω_c^0 states decaying to $\Xi_c^+ K^-$ in pp collisions at $\sqrt{s} = 7, 13$ TeV, *Phys. Rev. C* **102**, 054319 (2020).
- [19] S. Hu, G. Meng, and F. Xu, Hadronic weak decays of the charmed baryon Ω_c , *Phys. Rev. D* **101**, 094033 (2020).
- [20] H.-M. Yang and H.-X. Chen, P -wave charmed baryons of the $SU(3)$ flavor 6_F , *Phys. Rev. D* **104**, 034037 (2021).
- [21] A. Ramirez Morales, Strong decay widths and mass spectra of charmed baryons, Proc. Sci., ICHEP2022 (2022) 913, <https://pos.sissa.it/414/913>.
- [22] V. R. Debastiani, J. M. Dias, W. H. Liang, and E. Oset, Molecular Ω_c states generated from coupled meson-baryon channels, *Phys. Rev. D* **97**, 094035 (2018).
- [23] G. Montaña, A. Feijoo, and A. Ramos, A meson-baryon molecular interpretation for some Ω_c excited states, *Eur. Phys. J. A* **54**, 64 (2018).
- [24] A. Ramos, A. Feijoo, Q. Llorens, and G. Montaña, The molecular nature of some exotic hadrons, *Few Body Syst.* **61**, 34 (2020).
- [25] C. S. An and H. Chen, Observed Ω_c^0 resonances as pentaquark states, *Phys. Rev. D* **96**, 034012 (2017).
- [26] H.-J. Wang, Z.-Y. Di, and Z.-G. Wang, Analysis of the excited Ω_c states as the $\frac{1}{2}^\pm$ pentaquark states with QCD sum rules, *Commun. Theor. Phys.* **73**, 035201 (2021).
- [27] M. Padmanath and N. Mathur, Quantum Numbers of Recently Discovered Ω_c^0 Baryons from Lattice QCD, *Phys. Rev. Lett.* **119**, 042001 (2017).
- [28] R. Aaij *et al.*, The LHCb trigger and its performance in 2011, *J. Instrum.* **8**, P04022 (2013).
- [29] R. Aaij *et al.*, Design and performance of the LHCb trigger and full real-time reconstruction in Run 2 of the LHC, *J. Instrum.* **14**, P04013 (2019).
- [30] A. A. Alves Jr. *et al.* (LHCb Collaboration), The LHCb detector at the LHC, *J. Instrum.* **3**, S08005 (2008).
- [31] R. Aaij *et al.* (LHCb Collaboration), LHCb detector performance, *Int. J. Mod. Phys. A* **30**, 1530022 (2015).

- [32] T. Sjöstrand, S. Mrenna, and P. Skands, A brief introduction to PYTHIA 8.1, *Comput. Phys. Commun.* **178**, 852 (2008).
- [33] I. Belyaev *et al.* (LHCb Collaboration), Handling of the generation of primary events in Gauss, the LHCb simulation framework, *J. Phys. Conf. Ser.* **331**, 032047 (2011).
- [34] D. J. Lange, The EvtGen particle decay simulation package, *Nucl. Instrum. Methods Phys. Res., Sect. A* **462**, 152 (2001).
- [35] J. Allison *et al.* (Geant4 Collaboration), Geant4 developments and applications, *IEEE Trans. Nucl. Sci.* **53**, 270 (2006).
- [36] M. Clemencic, G. Corti, S. Easo, C. R. Jones, S. Miglioranza, M. Pappagallo, and P. Robbe (LHCb Collaboration), The LHCb simulation application, Gauss: Design, evolution and experience, *J. Phys. Conf. Ser.* **331**, 032023 (2011).
- [37] R. L. Workman *et al.* (Particle Data Group), Review of particle physics, *Prog. Theor. Exp. Phys.* **2022**, 083C01 (2022).
- [38] V. V. Gligorov and M. Williams, Efficient, reliable and fast high-level triggering using a bonsai boosted decision tree, *J. Instrum.* **8**, P02013 (2013).
- [39] A. Hoecker *et al.*, TMVA 4—toolkit for multivariate data analysis with ROOT, users guide, [arXiv:physics/0703039](https://arxiv.org/abs/physics/0703039).
- [40] G. A. Cowan, D. C. Craik, and M. D. Needham, RapidSim: An application for the fast simulation of heavy-quark hadron decays, *Comput. Phys. Commun.* **214**, 239 (2017).
- [41] J. M. Blatt and V. F. Weisskopf, *Theoretical Nuclear Physics* (Springer, New York, 1952), 10.1007/978-1-4612-9959-2.
- [42] R. Aaij *et al.* (LHCb Collaboration), Measurements of the Λ_b^0 , Ξ_b^- , and Ω_b^- Baryon Masses, *Phys. Rev. Lett.* **110**, 182001 (2013).
- [43] R. Aaij *et al.* (LHCb Collaboration), Precision measurement of D meson mass differences, *J. High Energy Phys.* **06** (2013) 065.
- [44] R. Aaij *et al.* (LHCb Collaboration), Precision Measurement of the Mass and Lifetime of the Ξ_b^- Baryon, *Phys. Rev. Lett.* **113**, 242002 (2014).

R. Aaij³², A. S. W. Abdelmotteleb⁵⁰, C. Abellan Beteta⁴⁴, F. Abudinén⁵⁰, T. Ackernley⁵⁴, B. Adeva⁴⁰, M. Adinolfi⁴⁸, P. Adlarson⁷⁷, H. Afsharnia⁹, C. Agapopoulou¹³, C. A. Aidala⁷⁸, Z. Ajaltouni⁹, S. Akar⁵⁹, K. Akiba³², P. Albicocco²³, J. Albrecht¹⁵, F. Alessio⁴², M. Alexander⁵³, A. Alfonso Albero³⁹, Z. Aliouche⁵⁶, P. Alvarez Cartelle⁴⁹, R. Amalric¹³, S. Amato², J. L. Amey⁴⁸, Y. Amhis^{11,42}, L. An⁴², L. Anderlini²², M. Andersson⁴⁴, A. Andreianov³⁸, M. Andreotti²¹, D. Andreou⁶², D. Ao⁶, F. Archilli^{31,b}, A. Artamonov³⁸, M. Artuso⁶², E. Aslanides¹⁰, M. Atzeni⁴⁴, B. Audurier¹², I. B. Bachiller Perea⁸, S. Bachmann¹⁷, M. Bachmayer⁴³, J. J. Back⁵⁰, A. Bailly-reyre¹³, P. Baladron Rodriguez⁴⁰, V. Balagura¹², W. Baldini^{21,42}, J. Baptista de Souza Leite¹, M. Barbetti^{22,c}, R. J. Barlow⁵⁶, S. Barsuk¹¹, W. Barter⁵², M. Bartolini⁴⁹, F. Baryshnikov³⁸, J. M. Basels¹⁴, G. Bassi^{29,d}, B. Batsukh⁴, A. Battig¹⁵, A. Bay⁴³, A. Beck⁵⁰, M. Becker¹⁵, F. Bedeschi²⁹, I. B. Bediaga¹, A. Beiter⁶², S. Belin⁴⁰, V. Bellec⁴⁴, K. Belous³⁸, I. Belov³⁸, I. Belyaev³⁸, G. Benane¹⁰, G. Bencivenni²³, E. Ben-Haim¹³, A. Bereznoy³⁸, R. Bernet⁴⁴, S. Bernet Andres⁷⁶, D. Berninghoff¹⁷, H. C. Bernstein⁶², C. Bertella⁵⁶, A. Bertolin²⁸, C. Betancourt⁴⁴, F. Betti⁴², I. A. Bezshyiko⁴⁴, J. Bhom³⁵, L. Bian⁶⁸, M. S. Bieker¹⁵, N. V. Biesuz²¹, P. Billoir¹³, A. Biolchini³², M. Birch⁵⁵, F. C. R. Bishop⁴⁹, A. Bitadze⁵⁶, A. Bizzeti⁴⁹, M. P. Blago⁴⁹, T. Blake⁵⁰, F. Blanc⁴³, J. E. Blank¹⁵, S. Blusk⁶², D. Bobulska⁵³, J. A. Boelhauve¹⁵, O. Boente Garcia¹², T. Boettcher⁵⁹, A. Boldyrev³⁸, C. S. Bolognani⁷⁴, R. Bolzonella^{21,e}, N. Bondar^{38,42}, F. Borgato²⁸, S. Borghi⁵⁶, M. Borsato¹⁷, J. T. Borsuk³⁵, S. A. Bouchiba⁴³, T. J. V. Bowcock⁵⁴, A. Boyer⁴², C. Bozzi²¹, M. J. Bradley⁵⁵, S. Braun⁶⁰, A. Brea Rodriguez⁴⁰, J. Brodzicka³⁵, A. Brossa Gonzalo⁴⁰, J. Brown⁵⁴, D. Brundu²⁷, A. Buonauro⁴⁴, L. Buonincontri²⁸, A. T. Burke⁵⁶, C. Burr⁴², A. Bursche⁶⁶, A. Butkevich³⁸, J. S. Butter³², J. Buytaert⁴², W. Byczynski⁴², S. Cadeddu²⁷, H. Cai⁶⁸, R. Calabrese^{21,e}, L. Calefice¹⁵, S. Cali²³, M. Calvi^{26,f}, M. Calvo Gomez⁷⁶, P. Campana²³, D. H. Campora Perez⁷⁴, A. F. Campoverde Quezada⁶, S. Capelli^{26,f}, L. Capriotti²⁰, A. Carbone^{20,g}, R. Cardinale^{24,h}, A. Cardini²⁷, P. Carniti^{26,f}, L. Carus¹⁴, A. Casais Vidal⁴⁰, R. Caspary¹⁷, G. Casse⁵⁴, M. Cattaneo⁴², G. Cavallero^{55,42}, V. Cavallini^{21,e}, S. Celani⁴³, J. Cerasoli¹⁰, D. Cervenkov⁵⁷, A. J. Chadwick⁵⁴, I. Chahrour⁷⁸, M. G. Chapman⁴⁸, M. Charles¹³, Ph. Charpentier⁴², C. A. Chavez Barajas⁵⁴, M. Chefdeville⁸, C. Chen¹⁰, S. Chen⁴, A. Chernov³⁵, S. Chernyshenko⁴⁶, V. Chobanova⁴⁰, S. Cholak⁴³, M. Chrzaszcz³⁵, A. Chubykin³⁸, V. Chulikov³⁸, P. Ciambone²³, M. F. Cicala⁵⁰, X. Cid Vidal⁴⁰, G. Ciezarek⁴², P. Cifra⁴², G. Ciullo^{21,e}, P. E. L. Clarke⁵², M. Clemencic⁴², H. V. Cliff⁴⁹, J. Closier⁴², J. L. Cobbedick⁵⁶, V. Coco⁴², J. Cogan¹⁰, E. Cogneras⁹, L. Cojocariu³⁷, P. Collins⁴², T. Colombo⁴², L. Congedo¹⁹, A. Contu²⁷, N. Cooke⁴⁷, I. Corredoira⁴⁰, G. Corti⁴², B. Couturier⁴², D. C. Craik⁴⁴, M. Cruz Torres^{1,i}, R. Currie⁵², C. L. Da Silva⁶¹, S. Dadabaev³⁸, L. Dai⁶⁵, X. Dai⁵, E. Dall’Occo¹⁵, J. Dalseno⁴⁰, C. D’Ambrosio⁴², J. Daniel⁹, A. Danilina³⁸, P. d’Argent¹⁹, J. E. Davies⁵⁶, A. Davis⁵⁶, O. De Aguiar Francisco⁵⁶, J. de Boer⁴², K. De Bruyn⁷³, S. De Capua⁵⁶

M. De Cian⁴³ U. De Freitas Carneiro Da Graca¹ E. De Lucia²³ J. M. De Miranda¹ L. De Paula² M. De Serio^{19,j}
D. De Simone⁴⁴ P. De Simone²³ F. De Vellis¹⁵ J. A. de Vries⁷⁴ C. T. Dean⁶¹ F. Debernardis^{19,j} D. Decamp⁸
V. Dedu¹⁰ L. Del Buono¹³ B. Delaney⁵⁸ H.-P. Dembinski¹⁵ V. Denysenko⁴⁴ O. Deschamps⁹ F. Dettori^{27,k}
B. Dey⁷¹ P. Di Nezza²³ I. Diachkov³⁸ S. Didenko³⁸ L. Dieste Maronas⁴⁰ S. Ding⁶² V. Dobishuk⁴⁶
A. Dolmatov³⁸ C. Dong³ A. M. Donohoe¹⁸ F. Dordei²⁷ A. C. dos Reis¹ L. Douglas⁵³ A. G. Downes⁸
P. Duda⁷⁵ M. W. Dudek³⁵ L. Dufour⁴² V. Duk⁷² P. Durante⁴² M. M. Duras⁷⁵ J. M. Durham⁶¹ D. Dutta⁵⁶
A. Dziurda³⁵ A. Dzyuba³⁸ S. Easo⁵¹ U. Egede⁶³ V. Egorychev³⁸ C. Eirea Orro⁴⁰ S. Eisenhardt⁵² E. Ejopu⁵⁶
S. Ek-In⁴³ L. Eklund⁷⁷ M. E Elashri⁵⁹ J. Ellbracht¹⁵ S. Ely⁵⁵ A. Ene³⁷ E. Epple⁵⁹ S. Escher¹⁴
J. Eschle⁴⁴ S. Esen⁴⁴ T. Evans⁵⁶ F. Fabiano^{27,k} L. N. Falcao¹ Y. Fan⁶ B. Fang^{11,68} L. Fantini^{72,l}
M. Faria⁴³ S. Farry⁵⁴ D. Fazzini^{26,f} L. F Felkowski⁷⁵ M. Feo⁴² M. Fernandez Gomez⁴⁰ A. D. Fernez⁶⁰
F. Ferrari²⁰ L. Ferreira Lopes⁴³ F. Ferreira Rodrigues² S. Ferreres Sole³² M. Ferrillo⁴⁴ M. Ferro-Luzzi⁴²
S. Filippov³⁸ R. A. Fini¹⁹ M. Fiorini^{21,e} M. Firlej³⁴ K. M. Fischer⁵⁷ D. S. Fitzgerald⁷⁸ C. Fitzpatrick⁵⁶
T. Fiutowski³⁴ F. Fleuret¹² M. Fontana¹³ F. Fontanelli^{24,h} R. Forty⁴² D. Foulds-Holt⁴⁹ V. Franco Lima⁵⁴
M. Franco Sevilla⁶⁰ M. Frank⁴² E. Franzoso^{21,e} G. Frau¹⁷ C. Frei⁴² D. A. Friday⁵⁶ L. Frontini^{25,m} J. Fu⁶
Q. Fuehring¹⁵ T. Fulghesu¹³ E. Gabriel³² G. Galati^{19,j} M. D. Galati³² A. Gallas Torreira⁴⁰ D. Galli^{20,g}
S. Gambetta^{52,42} M. Gandelman² P. Gandini²⁵ H. G Gao⁶ Y. Gao⁷ Y. Gao⁵ M. Garau^{27,k}
L. M. Garcia Martin⁵⁰ P. Garcia Moreno³⁹ J. Garcia Pardiñas⁴² B. Garcia Plana⁴⁰ F. A. Garcia Rosales¹²
L. Garrido³⁹ C. Gaspar⁴² R. E. Geertsema³² D. Gerick¹⁷ L. L. Gerken¹⁵ E. Gersabeck⁵⁶ M. Gersabeck⁵⁶
T. Gershon⁵⁰ L. Giambastiani²⁸ V. Gibson⁴⁹ H. K. Giemza³⁶ A. L. Gilman⁵⁷ M. Giovannetti^{23,b}
A. Gioventù⁴⁰ P. Gironella Gironell³⁹ C. Giugliano^{21,e} M. A. Giza³⁵ K. Gizdov⁵² E. L. Gkougkousis⁴²
V. V. Gligorov^{13,42} C. Göbel⁶⁴ E. Golobardes⁷⁶ D. Golubkov³⁸ A. Golutvin^{55,38} A. Gomes^{1,2,a,n,o}
S. Gomez Fernandez³⁹ F. Goncalves Abrantes⁵⁷ M. Goncerz³⁵ G. Gong³ I. V. Gorelov³⁸ C. Gotti²⁶
J. P. Grabowski⁷⁰ T. Grammatico¹³ L. A. Granado Cardoso⁴² E. Graugés³⁹ E. Graverini⁴³ G. Graziani⁴⁹
A. T. Greco³⁷ L. M. Greeven³² N. A. Grieser⁵⁹ L. Grillo⁵³ S. Gromov³⁸ B. R. Gruberg Cazon⁵⁷ C. Gu³
M. Guarise^{21,e} M. Guittiere¹¹ P. A. Günther¹⁷ E. Gushchin³⁸ A. Guth¹⁴ Y. Guz^{5,38} T. Gys⁴²
T. Hadavizadeh⁶³ C. Hadjivasiliou⁶⁰ G. Haefeli⁴³ C. Haen⁴² J. Haimberger⁴² S. C. Haines⁴⁹
T. Halewood-leagas⁵⁴ M. M. Halvorsen⁴² P. M. Hamilton⁶⁰ J. Hammerich⁵⁴ Q. Han⁷ X. Han¹⁷
S. Hansmann-Menzemer¹⁷ L. Hao⁶ N. Harnew⁵⁷ T. Harrison⁵⁴ C. Hasse⁴² M. Hatch⁴² J. He^{6,p}
K. Heijhoff³² F. H Hemmer⁴² C. Henderson⁵⁹ R. D. L. Henderson^{63,50} A. M. Hennequin⁵⁸ K. Hennessy⁵⁴
L. Henry⁴² J. Herd⁵⁵ J. Heuel¹⁴ A. Hicheur² D. Hill⁴³ M. Hilton⁵⁶ S. E. Hollitt¹⁵ J. Horswill⁵⁶ R. Hou⁷
Y. Hou⁸ J. Hu¹⁷ J. Hu⁶⁶ W. Hu⁵ X. Hu³ W. Huang⁶ X. Huang⁶⁸ W. Hulsbergen³² R. J. Hunter⁵⁰
M. Hushchyn³⁸ D. Hutchcroft⁵⁴ P. Ibis¹⁵ M. Idzik³⁴ D. Ilin³⁸ P. Ilten⁵⁹ A. Inglese³⁸ A. Iniukhin³⁸
A. Ishteev³⁸ K. Ivshin³⁸ R. Jacobsson⁴² H. Jage¹⁴ S. J. Jaimes Elles⁴¹ S. Jakobsen⁴² E. Jans³²
B. K. Jashal⁴¹ A. Jawahery⁶⁰ V. Jevtic¹⁵ E. Jiang⁶⁰ X. Jiang^{4,6} Y. Jiang⁶ M. John⁵⁷ D. Johnson⁵⁸
C. R. Jones⁴⁹ T. P. Jones⁵⁰ S. J Joshi³⁶ B. Jost⁴² N. Jurik⁴² I. Juszczak³⁵ S. Kandybei⁴⁵ Y. Kang³
M. Karacson⁴² D. Karpenkov³⁸ M. Karpov³⁸ J. W. Kautz⁵⁹ F. Keizer⁴² D. M. Keller⁶² M. Kenzie⁵⁰
T. Ketel³² B. Khanji¹⁵ A. Kharisova³⁸ S. Kholodenko³⁸ G. Khreich¹¹ T. Kim¹⁴ V. S. Kirsebom⁴³
O. Kitouni⁵⁸ S. Klaver³³ N. Kleijne^{29,d} K. Klimaszewski³⁶ M. R. Kmiec³⁶ S. Koliiev⁴⁶ L. Kolk¹⁵
A. Kondybayeva³⁸ A. Konoplyannikov³⁸ P. Kopciwicz³⁴ R. Kopecna¹⁷ P. Koppenburg³² M. Korolev³⁸
I. Kostiuk³² O. Kot⁴⁶ S. Kotriakhova³⁸ A. Kozachuk³⁸ P. Kravchenko³⁸ L. Kravchuk³⁸ R. D. Krawczyk⁴²
M. Kreps⁵⁰ S. Kretschmar¹⁴ P. Krokovny³⁸ W. Krupa³⁴ W. Krzemien³⁶ J. Kubat¹⁷ S. Kubis⁷⁵
W. Kucewicz³⁵ M. Kucharczyk³⁵ V. Kudryavtsev³⁸ E. K Kulikova³⁸ A. Kupsc⁷⁷ D. Lacarrere⁴²
G. Lafferty⁵⁶ A. Lai²⁷ A. Lampis^{27,k} D. Lancierini⁴⁴ C. Landesa Gomez⁴⁰ J. J. Lane⁵⁶ R. Lane⁴⁸
C. Langenbruch¹⁴ J. Langer¹⁵ O. Lantwin³⁸ T. Latham⁵⁰ F. Lazzari^{29,q} M. Lazzaroni^{25,m} C. Lazzeroni⁴⁷
R. Le Gac¹⁰ S. H. Lee⁷⁸ R. Lefèvre⁹ A. Leflat³⁸ S. Legotin³⁸ P. Lenisa^{21,e} O. Leroy¹⁰ T. Lesiak³⁵
B. Leverington¹⁷ A. Li³ H. Li⁶⁶ K. Li⁷ P. Li⁴² P.-R. Li⁶⁷ S. Li⁷ T. Li⁴ T. Li⁶⁶ Y. Li⁴ Z. Li⁶²
X. Liang⁶² C. Lin⁶ T. Lin⁵¹ R. Lindner⁴² V. Lisovskyi¹⁵ R. Litvinov^{27,k} G. Liu⁶⁶ H. Liu⁶ K. Liu⁶⁷
Q. Liu⁶ S. Liu^{4,6} A. Lobo Salvia³⁹ A. Loi²⁷ R. Lollini⁷² J. Lomba Castro⁴⁰ I. Longstaff⁵³ J. H. Lopes²
A. Lopez Huertas³⁹ S. López Soliño⁴⁰ G. H. Lovell⁴⁹ Y. Lu^{4,r} C. Lucarelli^{22,c} D. Lucchesi^{28,s} S. Luchuk³⁸

M. Lucio Martinez⁷⁴, V. Lukashenko^{32,46}, Y. Luo³, A. Lupato⁵⁶, E. Luppi^{21,e}, A. Lusiani^{29,d}, K. Lynch¹⁸, X.-R. Lyu⁶, R. Ma⁶, S. Maccolini¹⁵, F. Machefer¹¹, F. Maciuc³⁷, I. Mackay⁵⁷, V. Macko⁴³, L. R. Madhan Mohan⁴⁹, A. Maevskiy³⁸, D. Maisuzenko³⁸, M. W. Majewski³⁴, J. J. Malczewski³⁵, S. Malde⁵⁷, B. Malecki^{35,42}, A. Malinin³⁸, T. Maltsev³⁸, G. Manca^{27,k}, G. Mancinelli¹⁰, C. Mancuso^{11,25,m}, R. Manera Escalero³⁹, D. Manuzzi²⁰, C. A. Manzari⁴⁴, D. Marangotto^{25,m}, J. F. Marchand⁸, U. Marconi²⁰, S. Mariani^{22,c}, C. Marin Benito³⁹, J. Marks¹⁷, A. M. Marshall⁴⁸, P. J. Marshall⁵⁴, G. Martelli^{72,1}, G. Martellotti³⁰, L. Martinazzoli^{42,f}, M. Martinelli^{26,f}, D. Martinez Santos⁴⁰, F. Martinez Vidal⁴¹, A. Massafferri¹, M. Materok¹⁴, R. Matev⁴², A. Mathad⁴⁴, V. Matiunin³⁸, C. Matteuzzi²⁶, K. R. Mattioli¹², A. Mauri⁵⁵, E. Maurice¹², J. Mauricio³⁹, M. Mazurek⁴², M. McCann⁵⁵, L. Mcconnell¹⁸, T. H. McGrath⁵⁶, N. T. McHugh⁵³, A. McNab⁵⁶, R. McNulty¹⁸, B. Meadows⁵⁹, G. Meier¹⁵, D. Melnychuk³⁶, S. Meloni^{26,f}, M. Merk^{32,74}, A. Merli^{25,m}, L. Meyer Garcia², D. Miao^{4,6}, M. Mikhasenko^{70,t}, D. A. Milanese⁶⁹, E. Millard⁵⁰, M. Milovanovic⁴², M.-N. Minard^{8,a}, A. Minotti^{26,f}, T. Miralles⁹, S. E. Mitchell⁵², B. Mitreska¹⁵, D. S. Mitzel¹⁵, A. Modak⁵¹, A. Mödden¹⁵, R. A. Mohammed⁵⁷, R. D. Moise¹⁴, S. Mokhnenko³⁸, T. Mombächer⁴⁰, M. Monk^{50,63}, I. A. Monroy⁶⁹, S. Monteil⁹, G. Morello²³, M. J. Morello^{29,d}, M. P. Morgenthaler¹⁷, J. Moron³⁴, A. B. Morris⁴², A. G. Morris⁵⁰, R. Mountain⁶², H. Mu³, E. Muhammad⁵⁰, F. Muheim⁵², M. Mulder⁷³, K. Müller⁴⁴, C. H. Murphy⁵⁷, D. Murray⁵⁶, R. Murta⁵⁵, P. Muzzetto^{27,k}, P. Naik⁴⁸, T. Nakada⁴³, R. Nandakumar⁵¹, T. Nanut⁴², I. Nasteva², M. Needham⁵², N. Neri^{25,m}, S. Neubert⁷⁰, N. Neufeld⁴², P. Neustroev³⁸, R. Newcombe⁵⁵, J. Nicolini^{15,11}, D. Nicotra⁷⁴, E. M. Niel⁴³, S. Nieswand¹⁴, N. Nikitin³⁸, N. S. Nolte⁵⁸, C. Normand^{8,27,k}, J. Novoa Fernandez⁴⁰, G. N Nowak⁵⁹, C. Nunez⁷⁸, A. Oblakowska-Mucha³⁴, V. Obraztsov³⁸, T. Oeser¹⁴, S. Okamura^{21,e}, R. Oldeman^{27,k}, F. Oliva⁵², C. J. G. Onderwater⁷³, R. H. O'Neil⁵², J. M. Otorola Goicochea², T. Ovsianikova³⁸, P. Owen⁴⁴, A. Oyanguren⁴¹, O. Ozcelik⁵², K. O. Padeken⁷⁰, B. Pagare⁵⁰, P. R. Pais⁴², T. Pajero⁵⁷, A. Palano¹⁹, M. Palutan²³, G. Panshin³⁸, L. Paolucci⁵⁰, A. Papanestis⁵¹, M. Pappagallo^{19,j}, L. L. Pappalardo^{21,e}, C. Pappenheimer⁵⁹, W. Parker⁶⁰, C. Parkes⁵⁶, B. Passalacqua^{21,e}, G. Passaleva²², A. Pastore¹⁹, M. Patel⁵⁵, C. Patrignani^{20,g}, C. J. Pawley⁷⁴, A. Pellegrino³², M. Pepe Altarelli⁴², S. Perazzini²⁰, D. Pereima³⁸, A. Pereiro Castro⁴⁰, P. Perret⁹, K. Petridis⁴⁸, A. Petrolini^{24,h}, S. Petrucci⁵², M. Petruzzo²⁵, H. Pham⁶², A. Philippov³⁸, R. Piandani⁶, L. Pica^{29,d}, M. Piccini⁷², B. Pietrzyk⁸, G. Pietrzyk¹¹, M. Pili⁵⁷, D. Pinci³⁰, F. Pisani⁴², M. Pizzichemi^{26,42,f}, V. Placinta³⁷, J. Plews⁴⁷, M. Plo Casasus⁴⁰, F. Polci^{13,42}, M. Poli Lener²³, A. Poluektov¹⁰, N. Polukhina³⁸, I. Polyakov⁴², E. Polycarpo², S. Ponce⁴², D. Popov^{6,42}, S. Poslavskii³⁸, K. Prasanth³⁵, L. Promberger¹⁷, C. Prouve⁴⁰, V. Pugatch⁴⁶, V. Puill¹¹, G. Punzi^{29,q}, H. R. Qi³, W. Qian⁶, N. Qin³, S. Qu³, R. Quagliani⁴³, N. V. Raab¹⁸, B. Rachwal³⁴, J. H. Rademacker⁴⁸, R. Rajagopalan⁶², M. Rama²⁹, M. Ramos Pernas⁵⁰, M. S. Rangel², F. Ratnikov³⁸, G. Raven³³, M. Rebollo De Miguel⁴¹, F. Redi⁴², J. Reich⁴⁸, F. Reiss⁵⁶, C. Remon Alepuz⁴¹, Z. Ren³, P. K. Resmi⁵⁷, R. Ribatti^{29,d}, A. M. Ricci²⁷, S. Ricciardi⁵¹, K. Richardson⁵⁸, M. Richardson-Slipper⁵², K. Rinnert⁵⁴, P. Robbe¹¹, G. Robertson⁵², E. Rodrigues^{54,42}, E. Rodriguez Fernandez⁴⁰, J. A. Rodriguez Lopez⁶⁹, E. Rodriguez Rodriguez⁴⁰, D. L. Rolf⁴², A. Rollings⁵⁷, P. Roloff⁴², V. Romanovskiy³⁸, M. Romero Lamas⁴⁰, A. Romero Vidal⁴⁰, J. D. Roth^{78,a}, M. Rotondo²³, M. S. Rudolph⁶², T. Ruf⁴², R. A. Ruiz Fernandez⁴⁰, J. Ruiz Vidal⁴¹, A. Ryzhikov³⁸, J. Ryzka³⁴, J. J. Saborido Silva⁴⁰, N. Sagidova³⁸, N. Sahoo⁴⁷, B. Saitta^{27,k}, M. Salomoni⁴², C. Sanchez Gras³², I. Sanderswood⁴¹, R. Santacesaria³⁰, C. Santamarina Rios⁴⁰, M. Santimaria²³, E. Santovetti^{31,b}, D. Saranin³⁸, G. Sarpis¹⁴, M. Sarpis⁷⁰, A. Sarti³⁰, C. Satriano^{30,u}, A. Satta³¹, M. Saur¹⁵, D. Savrina³⁸, H. Sazak⁹, L. G. Scantlebury Smead⁵⁷, A. Scarabotto¹³, S. Schael¹⁴, S. Scherl⁵⁴, M. Schiller⁵³, H. Schindler⁴², M. Schmelling¹⁶, B. Schmidt⁴², S. Schmitt¹⁴, O. Schneider⁴³, A. Schopper⁴², M. Schubiger³², S. Schulte⁴³, M. H. Schune¹¹, R. Schwemmer⁴², B. Sciascia²³, A. Sciuccati⁴², S. Sellam⁴⁰, A. Semennikov³⁸, M. Senghi Soares³³, A. Sergi^{24,h}, N. Serra⁴⁴, L. Sestini²⁸, A. Seuthe¹⁵, Y. Shang⁵, D. M. Shangase⁷⁸, M. Shapkin³⁸, I. Shchemerov³⁸, L. Shchutska⁴³, T. Shears⁵⁴, L. Shekhtman³⁸, Z. Shen⁵, S. Sheng^{4,6}, V. Shevchenko³⁸, B. Shi⁶, E. B. Shields^{26,f}, Y. Shimizu¹¹, E. Shmanin³⁸, R. Shorkin³⁸, J. D. Shupperd⁶², B. G. Siddi^{21,e}, R. Silva Coutinho⁶², G. Simi²⁸, S. Simone^{19,j}, M. Singla⁶³, N. Skidmore⁵⁶, R. Skuza¹⁷, T. Skwarnicki⁶², M. W. Slater⁴⁷, J. C. Smallwood⁵⁷, J. G. Smeaton⁴⁹, E. Smith⁴⁴, K. Smith⁶¹, M. Smith⁵⁵, A. Snoch³², L. Soares Lavra⁹, M. D. Sokoloff⁵⁹, F. J. P. Soler⁵³, A. Solomin^{38,48}, A. Solovev³⁸, I. Solovyev³⁸, R. Song⁶³, F. L. Souza De Almeida², B. Souza De Paula², B. Spaan^{15,a}, E. Spadaro Norella^{25,m}, E. Spedicato²⁰

E. Spiridenkov,³⁸ P. Spradlin,⁵³ V. Sriskaran,⁴² F. Stagni,⁴² M. Stahl,⁴² S. Stahl,⁴² S. Stanislaus,⁵⁷ E. N. Stein,⁴² O. Steinkamp,⁴⁴ O. Stenyakin,³⁸ H. Stevens,¹⁵ D. Strelakina,³⁸ Y. S. Su,⁶ F. Suljik,⁵⁷ J. Sun,²⁷ L. Sun,⁶⁸ Y. Sun,⁶⁰ P. N. Swallow,⁴⁷ K. Swientek,³⁴ A. Szabelski,³⁶ T. Szumlak,³⁴ M. Szymanski,⁴² Y. Tan,³ S. Taneja,⁵⁶ M. D. Tat,⁵⁷ A. Terentev,⁴⁴ F. Teubert,⁴² E. Thomas,⁴² D. J. D. Thompson,⁴⁷ K. A. Thomson,⁵⁴ H. Tilquin,⁵⁵ V. Tisserand,⁹ S. T'Jampens,⁸ M. Tobin,⁴ L. Tomassetti,^{21,e} G. Tonani,^{25,m} X. Tong,⁵ D. Torres Machado,¹ D. Y. Tou,³ C. Trippel,⁴³ G. Tuci,⁶ N. Tuning,³² A. Ukleja,³⁶ D. J. Unverzagt,¹⁷ A. Usachov,³³ A. Ustyuzhanin,³⁸ U. Uwer,¹⁷ A. Vagner,³⁸ V. Vagnoni,²⁰ A. Valassi,⁴² G. Valenti,²⁰ N. Valls Canudas,⁷⁶ M. Van Dijk,⁴³ H. Van Hecke,⁶¹ E. van Herwijnen,⁵⁵ C. B. Van Hulse,^{40,v} M. van Veghel,³² R. Vazquez Gomez,³⁹ P. Vazquez Regueiro,⁴⁰ C. Vázquez Sierra,⁴² S. Vecchi,²¹ J. J. Velthuis,⁴⁸ M. Veltri,^{22,w} A. Venkateswaran,⁴³ M. Veronesi,³² M. Vesterinen,⁵⁰ D. Vieira,⁵⁹ M. Vieites Diaz,⁴³ X. Vilasis-Cardona,⁷⁶ E. Vilella Figueras,⁵⁴ A. Villa,²⁰ P. Vincent,¹³ F. C. Volle,¹¹ D. vom Bruch,¹⁰ A. Vorobyev,³⁸ V. Vorobyev,³⁸ N. Voropaev,³⁸ K. Vos,⁷⁴ C. Vrahas,⁵² J. Walsh,²⁹ E. J. Walton,⁶³ G. Wan,⁵ C. Wang,¹⁷ G. Wang,⁷ J. Wang,⁵ J. Wang,⁴ J. Wang,³ J. Wang,⁶⁸ M. Wang,²⁵ R. Wang,⁴⁸ X. Wang,⁶⁶ Y. Wang,⁷ Z. Wang,⁴⁴ Z. Wang,³ Z. Wang,⁶ J. A. Ward,^{50,63} N. K. Watson,⁴⁷ D. Websdale,⁵⁵ Y. Wei,⁵ B. D. C. Westhenry,⁴⁸ D. J. White,⁵⁶ M. Whitehead,⁵³ A. R. Wiederhold,⁵⁰ D. Wiedner,¹⁵ G. Wilkinson,⁵⁷ M. K. Wilkinson,⁵⁹ I. Williams,⁴⁹ M. Williams,⁵⁸ M. R. J. Williams,⁵² R. Williams,⁴⁹ F. F. Wilson,⁵¹ W. Wislicki,³⁶ M. Witek,³⁵ L. Witola,¹⁷ C. P. Wong,⁶¹ G. Wormser,¹¹ S. A. Wotton,⁴⁹ H. Wu,⁶² J. Wu,⁷ K. Wyllie,⁴² Z. Xiang,⁶ Y. Xie,⁷ A. Xu,⁵ J. Xu,⁶ L. Xu,³ L. Xu,³ M. Xu,⁵⁰ Q. Xu,⁶ Z. Xu,⁹ Z. Xu,⁶ D. Yang,³ S. Yang,⁶ X. Yang,⁵ Y. Yang,⁶ Z. Yang,⁵ Z. Yang,⁶⁰ L. E. Yeomans,⁵⁴ V. Yeroshenko,¹¹ H. Yeung,⁵⁶ H. Yin,⁷ J. Yu,⁶⁵ X. Yuan,⁶² E. Zaffaroni,⁴³ M. Zavertyaev,¹⁶ M. Zdybal,³⁵ M. Zeng,³ C. Zhang,⁵ D. Zhang,⁷ L. Zhang,³ S. Zhang,⁶⁵ S. Zhang,⁵ Y. Zhang,⁵ Y. Zhang,⁵⁷ Y. Zhao,¹⁷ A. Zharkova,³⁸ A. Zhelezov,¹⁷ Y. Zheng,⁶ T. Zhou,⁵ X. Zhou,⁷ Y. Zhou,⁶ V. Zhovkovska,¹¹ X. Zhu,³ X. Zhu,⁷ Z. Zhu,⁶ V. Zhukov,^{14,38} Q. Zou,^{4,6} S. Zucchelli,^{20,g} D. Zuliani,²⁸ and G. Zunica⁵⁶

(LHCb Collaboration)

¹Centro Brasileiro de Pesquisas Físicas (CBPF), Rio de Janeiro, Brazil

²Universidade Federal do Rio de Janeiro (UFRJ), Rio de Janeiro, Brazil

³Center for High Energy Physics, Tsinghua University, Beijing, China

⁴Institute Of High Energy Physics (IHEP), Beijing, China

⁵School of Physics State Key Laboratory of Nuclear Physics and Technology, Peking University, Beijing, China

⁶University of Chinese Academy of Sciences, Beijing, China

⁷Institute of Particle Physics, Central China Normal University, Wuhan, Hubei, China

⁸Université Savoie Mont Blanc, CNRS, IN2P3-LAPP, Annecy, France

⁹Université Clermont Auvergne, CNRS/IN2P3, LPC, Clermont-Ferrand, France

¹⁰Aix Marseille Univ, CNRS/IN2P3, CPPM, Marseille, France

¹¹Université Paris-Saclay, CNRS/IN2P3, IJCLab, Orsay, France

¹²Laboratoire Leprince-Ringuet, CNRS/IN2P3, Ecole Polytechnique, Institut Polytechnique de Paris, Palaiseau, France

¹³LPNHE, Sorbonne Université, Paris Diderot Sorbonne Paris Cité, CNRS/IN2P3, Paris, France

¹⁴I. Physikalisches Institut, RWTH Aachen University, Aachen, Germany

¹⁵Fakultät Physik, Technische Universität Dortmund, Dortmund, Germany

¹⁶Max-Planck-Institut für Kernphysik (MPIK), Heidelberg, Germany

¹⁷Physikalisches Institut, Ruprecht-Karls-Universität Heidelberg, Heidelberg, Germany

¹⁸School of Physics, University College Dublin, Dublin, Ireland

¹⁹INFN Sezione di Bari, Bari, Italy

²⁰INFN Sezione di Bologna, Bologna, Italy

²¹INFN Sezione di Ferrara, Ferrara, Italy

²²INFN Sezione di Firenze, Firenze, Italy

²³INFN Laboratori Nazionali di Frascati, Frascati, Italy

²⁴INFN Sezione di Genova, Genova, Italy

²⁵INFN Sezione di Milano, Milano, Italy

²⁶INFN Sezione di Milano-Bicocca, Milano, Italy

²⁷INFN Sezione di Cagliari, Monserrato, Italy

- ²⁸*Università degli Studi di Padova, Università e INFN, Padova, Padova, Italy*
- ²⁹*INFN Sezione di Pisa, Pisa, Italy*
- ³⁰*INFN Sezione di Roma La Sapienza, Roma, Italy*
- ³¹*INFN Sezione di Roma Tor Vergata, Roma, Italy*
- ³²*Nikhef National Institute for Subatomic Physics, Amsterdam, Netherlands*
- ³³*Nikhef National Institute for Subatomic Physics and VU University Amsterdam, Amsterdam, Netherlands*
- ³⁴*AGH - University of Science and Technology, Faculty of Physics and Applied Computer Science, Kraków, Poland*
- ³⁵*Henryk Niewodniczanski Institute of Nuclear Physics Polish Academy of Sciences, Kraków, Poland*
- ³⁶*National Center for Nuclear Research (NCBJ), Warsaw, Poland*
- ³⁷*Horia Hulubei National Institute of Physics and Nuclear Engineering, Bucharest-Magurele, Romania*
- ³⁸*Affiliated with an institute covered by a cooperation agreement with CERN*
- ³⁹*ICCUB, Universitat de Barcelona, Barcelona, Spain*
- ⁴⁰*Instituto Galego de Física de Altas Enerxías (IGFAE), Universidade de Santiago de Compostela, Santiago de Compostela, Spain*
- ⁴¹*Instituto de Física Corpuscular, Centro Mixto Universidad de Valencia - CSIC, Valencia, Spain*
- ⁴²*European Organization for Nuclear Research (CERN), Geneva, Switzerland*
- ⁴³*Institute of Physics, Ecole Polytechnique Fédérale de Lausanne (EPFL), Lausanne, Switzerland*
- ⁴⁴*Physik-Institut, Universität Zürich, Zürich, Switzerland*
- ⁴⁵*NSC Kharkiv Institute of Physics and Technology (NSC KIPT), Kharkiv, Ukraine*
- ⁴⁶*Institute for Nuclear Research of the National Academy of Sciences (KINR), Kyiv, Ukraine*
- ⁴⁷*University of Birmingham, Birmingham, United Kingdom*
- ⁴⁸*H.H. Wills Physics Laboratory, University of Bristol, Bristol, United Kingdom*
- ⁴⁹*Cavendish Laboratory, University of Cambridge, Cambridge, United Kingdom*
- ⁵⁰*Department of Physics, University of Warwick, Coventry, United Kingdom*
- ⁵¹*STFC Rutherford Appleton Laboratory, Didcot, United Kingdom*
- ⁵²*School of Physics and Astronomy, University of Edinburgh, Edinburgh, United Kingdom*
- ⁵³*School of Physics and Astronomy, University of Glasgow, Glasgow, United Kingdom*
- ⁵⁴*Oliver Lodge Laboratory, University of Liverpool, Liverpool, United Kingdom*
- ⁵⁵*Imperial College London, London, United Kingdom*
- ⁵⁶*Department of Physics and Astronomy, University of Manchester, Manchester, United Kingdom*
- ⁵⁷*Department of Physics, University of Oxford, Oxford, United Kingdom*
- ⁵⁸*Massachusetts Institute of Technology, Cambridge, MA, United States*
- ⁵⁹*University of Cincinnati, Cincinnati, OH, United States*
- ⁶⁰*University of Maryland, College Park, MD, United States*
- ⁶¹*Los Alamos National Laboratory (LANL), Los Alamos, NM, United States*
- ⁶²*Syracuse University, Syracuse, NY, United States*
- ⁶³*School of Physics and Astronomy, Monash University, Melbourne, Australia*
(associated with Department of Physics, University of Warwick, Coventry, United Kingdom)
- ⁶⁴*Pontificia Universidade Católica do Rio de Janeiro (PUC-Rio), Rio de Janeiro, Brazil*
(associated with Universidade Federal do Rio de Janeiro (UFRJ), Rio de Janeiro, Brazil)
- ⁶⁵*Physics and Micro Electronic College, Hunan University, Changsha City, China*
(associated with Institute of Particle Physics, Central China Normal University, Wuhan, Hubei, China)
- ⁶⁶*Guangdong Provincial Key Laboratory of Nuclear Science, Guangdong-Hong Kong Joint Laboratory of Quantum Matter, Institute of Quantum Matter, South China Normal University, Guangzhou, China*
(associated with Center for High Energy Physics, Tsinghua University, Beijing, China)
- ⁶⁷*Lanzhou University, Lanzhou, China*
(associated with Institute of High Energy Physics (IHEP), Beijing, China)
- ⁶⁸*School of Physics and Technology, Wuhan University, Wuhan, China*
(associated with Center for High Energy Physics, Tsinghua University, Beijing, China)
- ⁶⁹*Departamento de Física, Universidad Nacional de Colombia, Bogota, Colombia*
(associated with LPNHE, Sorbonne Université, Paris Diderot Sorbonne Paris Cité, CNRS/IN2P3, Paris, France)
- ⁷⁰*Universität Bonn - Helmholtz-Institut für Strahlen und Kernphysik, Bonn, Germany*
(associated with Physikalisches Institut, Ruprecht-Karls-Universität Heidelberg, Heidelberg, Germany)
- ⁷¹*Eotvos Lorand University, Budapest, Hungary*
(associated with European Organization for Nuclear Research (CERN), Geneva, Switzerland)
- ⁷²*INFN Sezione di Perugia, Perugia, Italy*
(associated with INFN Sezione di Ferrara, Ferrara, Italy)
- ⁷³*Van Swinderen Institute, University of Groningen, Groningen, Netherlands*
(associated with Nikhef National Institute for Subatomic Physics, Amsterdam, Netherlands)
- ⁷⁴*Universiteit Maastricht, Maastricht, Netherlands*
(associated with Nikhef National Institute for Subatomic Physics, Amsterdam, Netherlands)

⁷⁵*Tadeusz Kosciuszko Cracow University of Technology, Cracow, Poland*
(associated with *Henryk Niewodniczanski Institute of Nuclear Physics Polish Academy of Sciences, Kraków, Poland*)
⁷⁶*DS4DS, La Salle, Universitat Ramon Llull, Barcelona, Spain*
(associated with *ICCUB, Universitat de Barcelona, Barcelona, Spain*)
⁷⁷*Department of Physics and Astronomy, Uppsala University, Uppsala, Sweden*
(associated with *School of Physics and Astronomy, University of Glasgow, Glasgow, United Kingdom*)
⁷⁸*University of Michigan, Ann Arbor, MI, United States*
(associated with *Syracuse University, Syracuse, NY, United States*)

^aDeceased.

^bAlso at Università di Roma Tor Vergata, Roma, Italy.

^cAlso at Università di Firenze, Firenze, Italy.

^dAlso at Scuola Normale Superiore, Pisa, Italy.

^eAlso at Università di Ferrara, Ferrara, Italy.

^fAlso at Università di Milano Bicocca, Milano, Italy.

^gAlso at Università di Bologna, Bologna, Italy.

^hAlso at Università di Genova, Genova, Italy.

ⁱAlso at Universidad Nacional Autónoma de Honduras, Tegucigalpa, Honduras.

^jAlso at Università di Bari, Bari, Italy.

^kAlso at Università di Cagliari, Cagliari, Italy.

^lAlso at Università di Perugia, Perugia, Italy.

^mAlso at Università degli Studi di Milano, Milano, Italy.

ⁿAlso at Universidade Federal do Triângulo Mineiro (UFMT), Uberaba-MG, Brazil.

^oAlso at Universidade de Brasília, Brasília, Brazil.

^pAlso at Hangzhou Institute for Advanced Study, UCAS, Hangzhou, China.

^qAlso at Università di Pisa, Pisa, Italy.

^rAlso at Central South U., Changsha, China.

^sAlso at Università di Padova, Padova, Italy.

^tAlso at Excellence Cluster ORIGINS, Munich, Germany.

^uAlso at Università della Basilicata, Potenza, Italy.

^vAlso at Universidad de Alcalá, Alcalá de Henares, Spain.

^wAlso at Università di Urbino, Urbino, Italy.